EUROPEAN ORGANIZATION FOR NUCLEAR RESEARCH

DIRAC Note 2016-04
May 23, 2016

The estimation of production rates of π^+K^-, π^-K^+ and $\pi^+\pi^-$ atoms in proton-nucleus interactions at 24 and 450 GeV/c

O.Gorchakov, L.Nemenov

GENEVA
2016

Abstract.

Short-lived ($\tau \sim 3 \times 10^{-15} s$) π^+K^-, $K^+\pi^-$ and $\pi^+\pi^-$ atoms as well as long-lived ($\tau \geq 1 \times 10^{-11}$ s) $\pi^+\pi^-$ atoms produced in proton-nucleus interactions at 24 GeV/c are observed and studied in the DIRAC experiment at the CERN PS. The purpose of this paper is to show that the yields of the short-lived π^+K^-, $K^+\pi^-$ and $\pi^+\pi^-$ atoms in proton-nucleus interactions at 450 GeV/c and $\theta_{lab} = 4^\circ$ are estimated to be, respectively, 17, 38 and 16 times higher. This may allow significantly improving the precision of their lifetime measurement and $\pi\pi$ and πK scattering length combinations $|a_0 - a_2|$ and $|a_{1/2} - a_{3/2}|$. The yields of the long-lived π^+K^-, $K^+\pi^-$ and $\pi^+\pi^-$ atoms at 450 GeV/c are estimated to be 180,800 and 370 times higher per time unit than at 24 GeV/c. This may allow the resonance method to be used for measuring the Lamb shift in the $\pi\pi$ atom and a new $\pi\pi$ scattering length combination $2a_0 + a_2$ to be obtained.

1. Introduction

The lifetime measurement of atoms consisting of K^+ and π^- ($A_{K\pi}$), K^- and π^+ ($A_{\pi K}$) and π^+ and π^- ($A_{2\pi}$) allows model-independent measurement of the $\pi\pi$ and $K\pi$ scattering lengths [1–4]. Experimental investigations of the $A_{K\pi}$ and $A_{2\pi}$ atoms were performed in the DIRAC experiment at the CERN PS at the proton beam momentum of 24 GeV/c [5–9]. In all these experiments the pairs of charged particles with small relative momentum Q in their c.m.s.(atomic pairs) generated after atom breakup in the target were detected.

The lifetime of short-lived $A_{2\pi}$ ($\tau_{th} = 2.9 \times 10^{-15} s$) is related to the $\pi\pi$ s-wave scattering length combination $|a_0 - a_2|$, where 0 and 2 are the isospin values. In the DIRAC experiment the τ was measured [6, 7] with a precision of about 9% which gives 4.3% for the $|a_0 - a_2|$ combination accuracy (statistical error 3.1%), far from the theoretical uncertainty of 1.5% [3] which can be improved using the latest results of lattice calculations.

The lifetime of short-lived $A_{\pi^+K^-}$ and $A_{K^+\pi^-}$ ($\tau_{th} = 3.5 \times 10^{-15} s$) is related to the πK s-wave scattering length combination $|a_{1/2} - a_{3/2}|$, where 1/2 and 3/2 are the isospin values. The limited number of the produced and detected short-lived $K\pi$ atoms allowed to estimate their lifetime and the $K\pi$ scattering length combination $|a_{1/2} - a_{3/2}|$ with the errors of 100% and 60% respectively [8]. The theoretical prediction of $K\pi$ scattering

lengths are obtained with the 6-10% error [10–13]. The measurement of the s-wave πK scattering lengths would test our understanding of the chiral symmetry breaking in processes with u, d and s quarks, while the measurement of $\pi\pi$ scattering lengths checks only the symmetry breaking in the processes with u and d quarks.

The investigation of long-lived $A_{2\pi}$ allows the Lamb shift to be measured in this atom [14–16] and another combination of the $\pi\pi$ scattering lengths $2a_0 + a_2$ to be extracted [4, 17, 18]. If the resonance method can be used, this combination will be obtained with a precision an order of magnitude higher than in other methods [7,19,20]. At the present time 436±61 $\pi^+\pi^-$ pairs generated in the breakup of long-lived $A_{2\pi}$ in the Pt foil have been observed in the DIRAC experiment [9].

In the present work the calculations are performed using the FTF generator [21], which is a developed version of FTITIOF generator for GEANT4 [22]. There are no experimental data on inclusive $\pi^\pm$ and $K^\pm$ production in pNi-interactions at 24 GeV/c. Therefore, to estimate the FTF precision in describing these data we compare the FTF predictions with the experimental data on inclusive $\pi^\pm$ and $K^\pm$ production in pC interactions at 31 GeV/c [23] (in the same angle and momentum intervals as in the DIRAC experiment). The experimental data from pC and pCu interactions at 100 GeV/c [24] are also compared with the generator predictions to make the conclusion about FTF ability to describe inclusive cross sections for both nuclei. The FTF accuracy at 450 GeV/c was checked only in the laboratory angle interval 0-1.7° where there are experimental data [25]. The absolute and relative dimesoatom yields at 450 GeV/c as a function of polar angle in laboratory system (l.s.) θ_{lab} and atom momentum are calculated. It allows obtaining the expected number of detected short-lived and long-lived dimesoatoms and possible statistical errors.

2. Basic relations

The atom production probability is proportional to the double inclusive cross section for generation of two constituent particles of this atom with small relative momenta. Calculating the atom production cross section, one should exclude the contribution to the double cross section from those constituents that arise from the decays of long-lived particles and cannot form the atom. When one or both particles in the pair come from these decays the typical range between them is much larger than the Bohr radius of the atom (249 fm for $A_{\pi K}$ and 387 fm for $A_{2\pi}$) and the atom production probability is negligible. The main long-lived sources of pions are η and η'. In the case of pions and kaons, the main contribution comes from the short-lived sources.

The laboratory differential inclusive cross section for the atom production can be written in the form [14]

$$\frac{d\sigma_n^A}{d\vec{p}_A} = (2\pi)^3 \frac{E_A}{M_A} |\Psi_n(0)|^2 \left. \frac{d^2\sigma_s}{d\vec{p}_1\, d\vec{p}_2} \right|_{\vec{p}_1=\frac{m_1}{m_2}\vec{p}_2=\frac{m_1}{M_A}\vec{p}_A}, \quad (1)$$

where M_A is the atom mass, $\vec{p}_A$ and E_A are the momentum and energy of the atom in

the l.s., respectively, $|\Psi_n(0)|^2 = p_B^3/\pi n^3$ is the atomic wave function (without regard for the strong interactions between the particles forming the atom, i.e., it is the pure Coulomb wave function) squared at the origin with the principal quantum number n and the orbital momentum $l = 0$, p_B is the Bohr momentum of the particles in the atom, $d^2\sigma_s^0/d\vec{p}_1 d\vec{p}_2$ is the double inclusive production cross section for the pairs from the short-lived sources (hadronization processes, ρ, ω, Δ, K^*, Σ^*, etc.) without regard for the $\pi^+\pi^-$ ($K^+\pi^-$, $K^-\pi^+$) Coulomb interaction in the final state, and $\vec{p}_1$ and $\vec{p}_2$ are the momenta of the particles forming the atom in the l.s.. The momenta obey the relation $\vec{p}_1 = \frac{m_1}{m_2}\vec{p}_2 = \frac{m_1}{M_A}\vec{p}_A$ (m_1 and m_2 are the masses of the particles). The atoms are produced with the orbital momentum $l = 0$, because $|\Psi_{n,l}(0)|^2 = 0$ when $l \neq 0$. The atoms are distributed over n as n^{-3}: $W_1 = 83\%$, $W_2 = 10.4\%$, $W_3 = 3.1\%$, $W_{n\geq 4} = 3.5\%$. Note that $\Sigma_{n=1}^{\infty}|\Psi_n(0)|^2 = 1.202|\Psi_1(0)|^2$.

After substituting the expression for $|\Psi_n(0)|^2$ and summing over n, one can obtain an expression for the inclusive cross sections of atom production in all s-states through the inclusive yields of positive and negative hadron pairs

$$\frac{d\sigma^A}{d\vec{p}_A} = 1.202 \times 8\,\pi^2\,(\mu\alpha)^3\,\frac{E_A}{M_A}\,\left.\frac{d^2\sigma_s}{d\vec{p}_1\,d\vec{p}_2}\right|_{\vec{p}_1=\frac{m_1}{m_2}\vec{p}_2=\frac{m_1}{M_A}\vec{p}_A}, \qquad (2)$$

where μ is the reduced mass of the atom ($\mu = \frac{m_1 m_2}{m_1+m_2}$), and α is the fine structure constant.

Instead of the differential cross section, it is convenient to introduce the particle production probability per inelastic interaction (yield)

$$\frac{dN}{d\vec{p}} = \frac{d\sigma}{d\vec{p}}\,\frac{1}{\sigma_{in}}, \qquad \frac{d^2N}{d\vec{p_1}d\vec{p_2}} = \frac{d^2\sigma}{d\vec{p_1}d\vec{p_2}}\,\frac{1}{\sigma_{in}}, \qquad (3)$$

where σ_{in} is the inelastic cross section of hadron production.

Then

$$\frac{dN_A}{d\vec{p}_A} = 1.202 \times 8\,\pi^2\,(\mu\alpha)^3\,\frac{E_A}{M_A}\,\left.\frac{d^2N_s}{d\vec{p}_1\,d\vec{p}_2}\right|_{\vec{p}_1=\frac{m_1}{m_2}\vec{p}_2=\frac{m_1}{M_A}\vec{p}_A}, \qquad (4)$$

The double yield (without regard for the Coulomb interaction) can be presented as [26]:

$$\frac{d^2N_s}{d\vec{p}_1 d\vec{p}_2} = \frac{dN_1}{d\vec{p}_1}\,\frac{dN_2}{d\vec{p}_2}\,R(\vec{p_1},\vec{p_2},s), \qquad (5)$$

where $dN_1/d\vec{p}_1$ and $dN_2/d\vec{p}_2$ are the single-particle yields, R is a correlation function due to strong interaction only, and s is the c.m.s. energy squared.

The $A_{2\pi}$ yield was measured [7] at 24 GeV/c and $\theta_{lab} = 5.7^\circ$, the yields of π^+K^- and $K^+\pi^-$ atoms at the same proton momentum and angle were obtained in [8]. Hence it is useful to present not only the absolute yields of the atoms at different conditions but also their yields relative to the known values.

3. Experimental values of pion and kaon inclusive cross sections and their description by FTF.

It is important to know how well the inclusive cross sections obtained by the FTF describe the corresponding experimental data at 24 and 450 GeV/c. The main pion momentum interval in $\pi^+\pi^-$ atomic pairs in the DIRAC experiment is 1-3 GeV/c, and for kaons from the $A_{\pi K}$ breakup it is 4-7 GeV/c. We are going to use Ni target but there is no data for pion and kaon inclusive cross sections for this material. The data [27] reveal the weak dependence of the soft pion and kaon yields on the nucleon atomic number A from Be to Cu. The weak dependence of these yields on A is also observed [24] in p-nucleus (C, Al, Cu) interactions at 100 GeV/c for the secondary particle momentum of 30 GeV/c. Therefore, the experimental soft particle yields in carbon and Be can be used to check the FTF precision, and then one may assume that the same degree of agreement of the FTF predictions with the data exists for pNi interactions.

3.1. Comparison of experimental inclusive cross sections in pC interactions at 31 GeV/c with FTF predictions.

The inclusive cross sections of π^+, π^-, K^+, and K^- in pC interactions at 31 GeV/c were measured with high precision and compared with the VENUS, EPOS and GiBUU predictions in [23]. The Figures 1 and 2 present the experimental and calculated inclusive yields of π^+, π^-, K^+, and K^- in this experiment as a function of the particle momentum in l.s. The intervals of the π^+ and π^- polar angle θ_{lab} in laboratory system (l.s.). from 60 to 100 mrad and from 100 to 140 mrad fully cover the θ_{lab} interval of the DIRAC setup (82-116 mrad). From Fig.1 we can see that the FTF predictions describe the inclusive cross sections in the momentum interval 1-3 GeV/c with an accuracy better than 10%.

For K^+ inclusive yields in a broad θ_{lab} interval of 20-140 mrad (Fig.2) the calculated values are 30% higher than the experimental ones.

For K^-, the calculated values in the interval 60-140 mrad are ≈15 % higher than the experimental data (Fig.2) at p_K =4 GeV/c and ≈100 % higher at p_K = 7 GeV/c. The mentioned above discrepancies between experimental and calculated inclusive cross sections at 24 GeV/c and 450 GeV/c (see paragraph 3.2) were taking in to account when the atoms yields ratios were calculated in chapter 5.

3.2. Comparison of experimental inclusive cross sections in p-Be interactions at 450 GeV/c and 100 GeV/c with FTF predictions.

The invariant inclusive cross sections of π^+, π^-, K^+ and K^- in pBe interactions at 450 GeV/c were measured in [25] and compared with FTF predictions in [29]. It was shown that the generator described well the inclusive cross sections of π^+ and π^- up to the momentum of 70 GeV/c (Fig.3, bottom). Therefore, the generator can be used for description of $A_{2\pi}$ yields up to the atom momentum of 140 GeV/c.

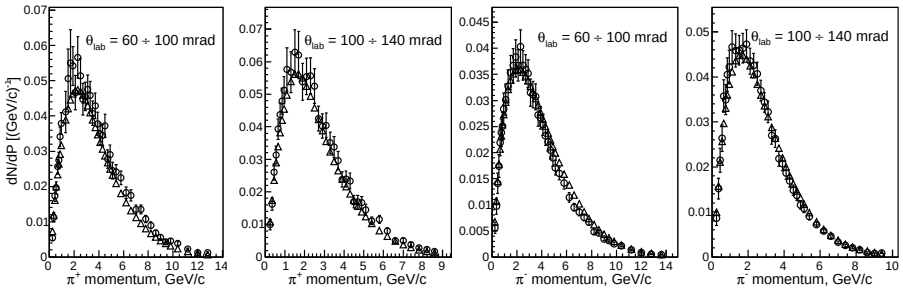

Figure 1. The yields of π^+ and π^- in pC interactions at 31 GeV/c for polar angles of 60-100 and 100-140 mrad. ○ - are the experimental data [23] and △ - are the FTF simulation data.

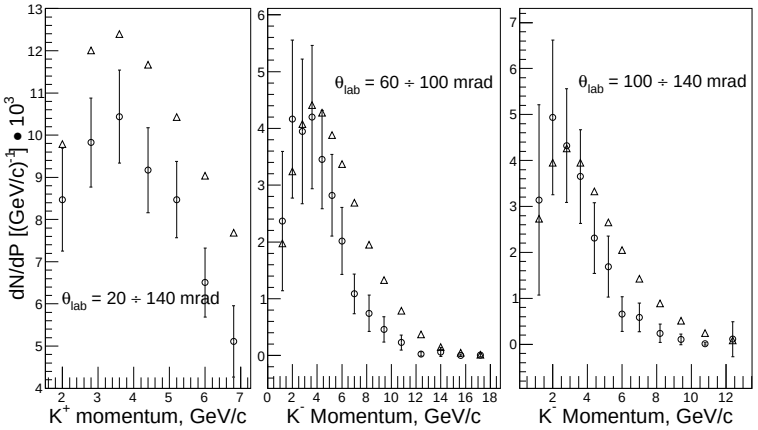

Figure 2. The yields of K^+ in pC interactions at 31 GeV/c for polar angles of 20-140 and K^- for angles 60-100 and 100-140 mrad. ○ - are the experimental data [23] and △ - are the FTF simulation data.

The inclusive cross sections of K mesons are described with an accuracy of about 20% up to the momentum of 20 GeV/c and 40 GeV/c for K^+ and K^- respectively (Fig.3, bottom). It allows the yields of $A_{K\pi}$ and $A_{\pi K}$ to be calculated up to the atom momentum of 26 GeV/c and 51 GeV/c respectively.

The data on the dependence of the experimental inclusive yields of the π and K mesons with the momenta of 15 GeV/c and 40 GeV/c on p_t are described [29] by the FTF well (Fig.3, top).

The data on the inclusive production of π^+, π^-, K^+, and K^- in the pC and pCu interactions at 100 GeV/c [24] were compared with the FTF predictions in [29]. It was shown that the FTF did not describe the experimental data at large x for the pC interactions. The disagreement between the FTF predictions and the experimental pCu data was smaller than for the pC interactions. It can be considered as the indication that the yield of dimesoatoms at 450 GeV/c with the Ni target can be described by the FTF not worse than with the Be target.

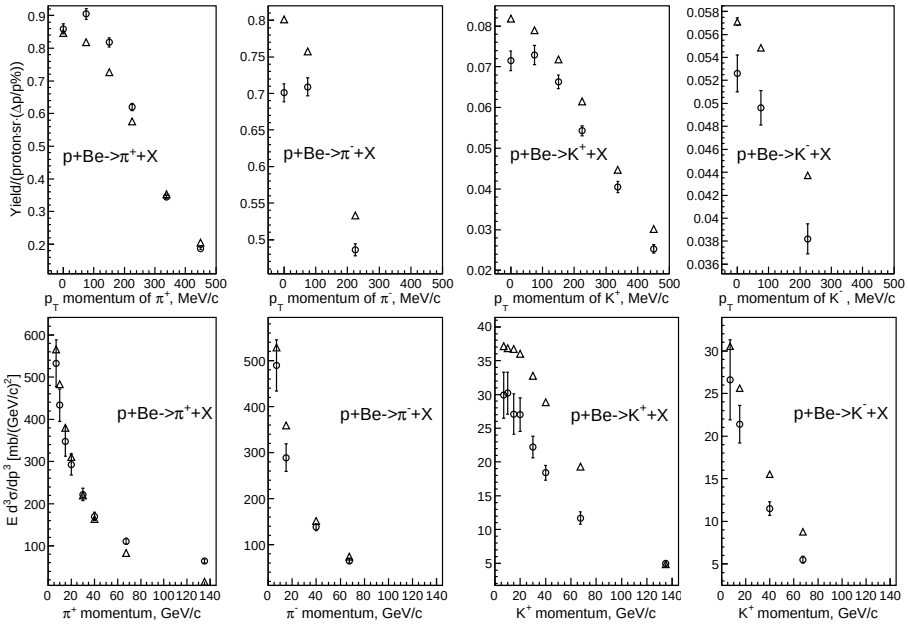

Figure 3. Top: the yields of π^+, π^-, K^+ and K^- in the pBe interactions at 450 GeV/c as a function of p_t. Bottom: the invariant inclusive cross sections of π^+, π^-, K^+ and K^- in the pBe interactions at 450 GeV/c as a function of the particle momentum in the forward direction. ○ - are the experimental data [23] and △ - are the FTF simulation data.

4. Results of calculations

The selection of particles from the long-lived and short-lived sources was performed. Further, using yields from the short-lived sources only we obtained the double inclusive yields of the $\pi^+\pi^-$, $K^+\pi^-$ and $K^-\pi^+$ pairs and the dependence of corresponding atom yields on their angle and momentum in laboratory system.

It is important to know the ratio between the number of the dimesoatoms and the full flux of the charged particles in the same solid angle, which is seven orders of magnitude higher than the number of atoms. This flux of the charged particles restricts the intensity of the primary proton beam and consequently the number of generated atoms per time unit. Therefore, the yield of charged particles was also calculated for each angle and proton momentum.

4.1. Calculations of inclusive yields of charged particles, $\pi\pi$ and πK atoms.

In this subsection the yield is calculated in the solid angle of $10^{-3}sr$ without allowance for the setup acceptance and particle decays.

Figure 4 shows the total yields of the charged particles ($\pi^{\pm}$, $K^{\pm}$, p and $\bar{p}$) per pNi interaction event at 450 GeV/c and an emission angles $\theta_{lab} = 0°$, $2°$, $4°$ (right) and at 24 GeV/c and an emission angle $\theta_{lab} = 5.7°$ (left) as a function of their momentum.

The yields of all the atoms into solid angle of 10^{-3} sr are shown at the top of

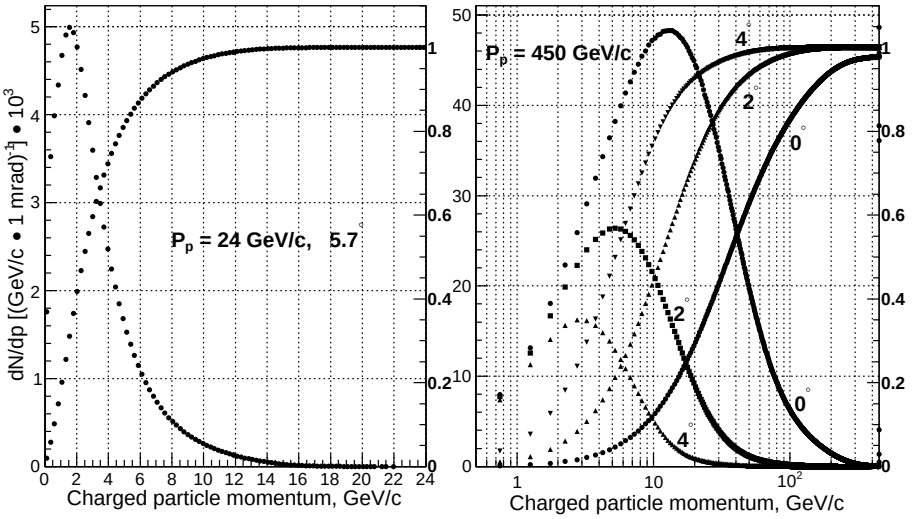

Figure 4. The total yield of the charged particles ($\pi^{\pm}$, $K^{\pm}$, p and $\bar{p}$) per pNi interaction event at 450 GeV/c and an emission angles $\theta_{lab} = 0°$, $2°$, $4°$ (right) and at 24 GeV/c and emission angle $\theta_{lab} = 5.7°$ (left) as a function of their momentum in l.s. for the solid angle of 10^{-3} sr. The integrated and normalized to 1 distributions are shown.

Fig.5. In the middle of Fig.5 the same yields of $A_{2\pi}$, $A_{\pi^+K^-}$ and $A_{K^+\pi^-}$ as a function of their momentum are presented in the intervals 2.5-10.5 GeV/c ($A_{2\pi}$) and 5-14 GeV/c ($A_{\pi K}$). The chosen intervals are the working intervals of the DIRAC setup in which identification of charged particle type is really simple.

Table 1 presents these yields integrated over p_A in the working intervals; W_{ch} and W_A are the total yields of the charged particles ($\pi^{\pm}$, $K^{\pm}$, p, $\bar{p}$) and the $\pi^+\pi^-$, π^+K^-, and $K^+\pi^-$ atoms respectively into the aperture of 10^{-3} sr per pNi interaction event at 450 and 24 GeV/c. The relative yields of the charged particles and atoms at 450 and 24 GeV/c are W^N_{ch}=$W_{ch}/W_{ch}(5.7°, 24\ GeV/c)$ and W^N_A=$W_A/W_A(5.7°, 24\ GeV/c)$). The yield of $A_{2\pi}$ and $A_{\pi K}$ are practically the same as in [30] where the FRITIOF 6 code was used for calculations.

The yields of the $\pi^+\pi^-$, π^+K^- and $K^+\pi^-$ atoms at $\theta_{lab} = 4°$ and at 450 GeV/c are 17, 37 and 16 times higher respectively than at 24 GeV/c and $\theta_{lab} = 5.7°$. These yields and the corresponding ratios at 450 GeV/c and $\theta_{lab} = 2°$ are twice as high again.

4.2. Calculations of inclusive yields of $\pi\pi$ and πK atoms detected by the setup

The acceptance of the DIRAC setup for πK and $\pi\pi$ atoms detection at 24 GeV/c without allowance for the particle decays is presented in Fig.6. We used the same acceptance at 450 GeV/c to obtain the yield that allows calculating the expected number of $A_{2\pi}$, $A_{\pi^+K^-}$ and $A_{K^+\pi^-}$ at 450 GeV/c using the DIRAC experimental data.

The yields of $A_{\pi^+K^-}$, $A_{K^+\pi^-}$ and $A_{2\pi}$ per pNi interaction event into solid angle of 10^{-3} sr with allowance for the setup acceptance are presented in Fig.5 (bottom) as

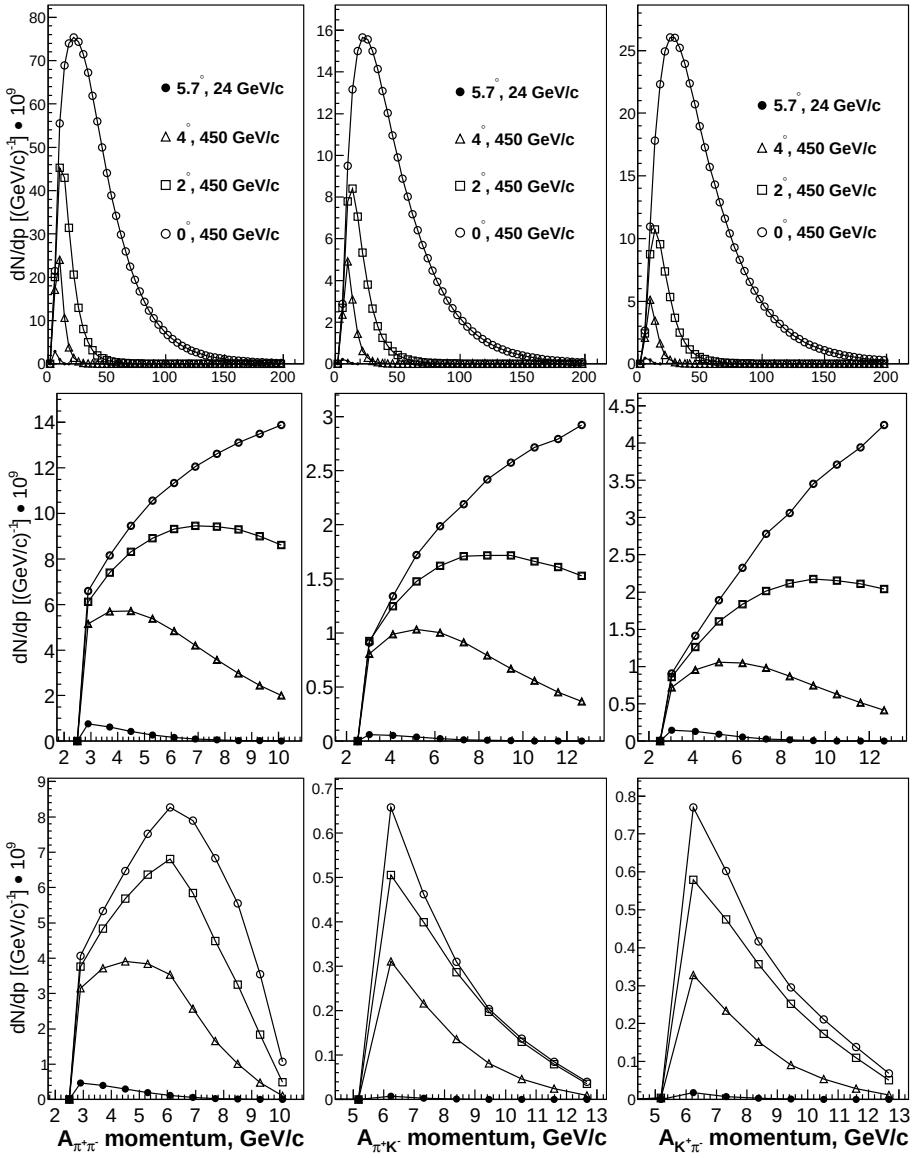

Figure 5. Yields of $A_{2\pi}$, $A_{\pi K}$ and $A_{K\pi}$ per pNi interaction event at 450 GeV/c and emission angles $\theta_{lab} = 0°$, $2°$, $4°$ and at 24 GeV/c and an emission angle $\theta_{lab} = 5.7°$ as a function of the atom momentum in l.s for the solid angle of 10^{-3} sr. Top: the DIRAC setup acceptance and decays of pions and kaons are ignored. Middle: the same distributions as on the top in the setup momentum interval. Bottom: the acceptance of the setup and the pion and kaon decays are taken into account.

● - $\theta_{lab} = 5.7°$, 24 GeV/c.

450 GeV/c: $\theta_{lab} = 0°(\bigcirc), 2°(\square), 4°(\triangle)$.

a function of the atom momentum. These yields integrated over p_A in the working intervals are shown in Table 2. together with the relative yields (the yield at 24 GeV/c and 5.7° is set to 1) and the yields relative to the flux of the charged particles. The latter values are important since the forward detectors should operate at this flux of the charged particles. Also this ratio is less sensitive to the accuracy of the meson

Table 1. The total yields of charged particles ($\pi^{\pm}$, $K^{\pm}$, p and $\bar{p}$) W_{ch} and the $\pi^+\pi^-$, π^+K^-, and $K^+\pi^-$ atoms W_A into the aperture of 10^{-3} sr per pNi interaction event at 24 and 450 GeV/c versus the emission angle θ_{lab} in the intervals 2.5-10.5 GeV/c ($A_{2\pi}$) and 5-14 GeV/c ($A_{\pi K}$) without allowance for the decays of pions and kaons in the setup. The relative yields of the charged particles and atoms are W_{ch}^N=$W_{ch}/W_{ch}(5.7^\circ, 24\ GeV/c)$ and W_A^N=$W_A/W_A(5.7^\circ, 24\ GeV/c)$.

θ_{lab}	5.7°	4°	2°	0°
p_p	24 GeV/c	450 GeV/c	450 GeV/c	450 GeV/c
Yield of charged particles				
W_{ch}	0.022	0.14	0.50	2.9
W_{ch}^N	1	6.4	22.7	132
Yield of $\pi^+\pi^-$ atoms				
$W_A \times 10^9$	1.94	34	69	89
W_A^N	1	17.3	35.4	45.9
Yield of π^+K^- atoms				
$W_A \times 10^9$	0.217	8.1	16.3	23
W_A^N	1	37.5	75.	106.
Yield of $K^+\pi^-$ atoms				
$W_A \times 10^9$	0.52	8.5	19	30
W_A^N	1	16.4	37.6	57.4

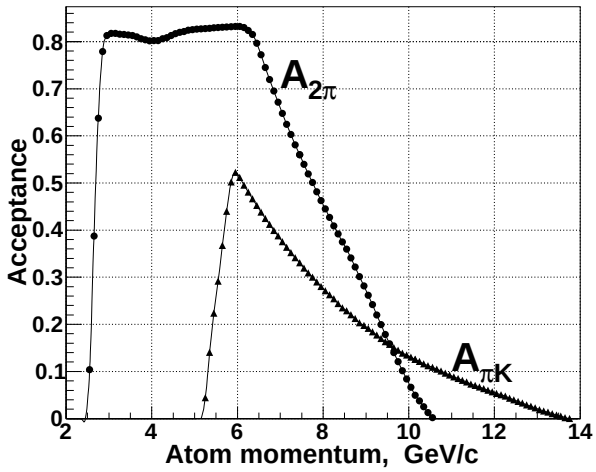

Figure 6. The acceptance of the DIRAC setup for $A_{2\pi}$ and $A_{\pi K}$ as a function of the atom momentum. Decays of pions and kaons are not taken into account.

production inclusive cross sections than the atomic absolute yield.

The yields of the $\pi^+\pi^-$, π^+K^- and $K^+\pi^-$ atoms at 450 GeV/c and $\theta_{lab} = 4^\circ$, where charged particle momenta are small and their identification is relatively simple, are 15, 67, and 31 times higher respectively than at 24 GeV/c and $\theta_{lab} = 5.7^\circ$. It means

Table 2. The yield of the $\pi^+\pi^-$, π^+K^- and $K^+\pi^-$ atoms W_A into the aperture of 10^{-3} *sr* with allowance for the setup acceptance and pion and kaon decays per pNi interaction event at 24 and 450 GeV/c versus the emission angle θ_{lab}. W_A^N=$W_A/W_A(5.7^\circ, 24\ GeV/c)$ and $(W_A/W_{ch})^N$=$(W_A/W_{ch})/((W_A/W_{ch})(5.7^\circ, 24\ GeV/c))$.

θ_{lab}	5.7°	4°	2°	0°
E_p	24 GeV/c	450 GeV/c	450 GeV/c	450 GeV
Yield of $\pi^+\pi^-$ atoms				
$W_A \times 10^9$	1.25	19	35	45
W_A^N	1	15	28	36
$W_A/W_{ch} \times 10^9$	57	140	70	16
$(W_A/W_{ch})^N$	1	2.4	1.2	0.27
Yield of π^+K^- atoms				
$W_A \times 10^9$	0.013	0.88	1.7	2.0
W_A^N	1	67	131	154
$W_A/W_{ch} \times 10^9$	0.59	6.3	3.4	0.69
$(W_A/W_{ch})^N$	1	10.6	5.8	1.2
Yield of $K^+\pi^-$ atoms				
$W_A \times 10^9$	0.031	0.97	2.1	2.7
W_A^N	1	31	68	87
$W_A/W_{ch} \times 10^9$	1.4	6.9	4.2	0.93
$(W_A/W_{ch})^N$	1.	4.9	3.0	0.66

that it is possible to decrease the proton beam intensity to reduce of trigger events with accidental coincidences. The additional increase in the atom production is connected with the beam time during the supercycle on the PS and SPS. The DIRAC experiment on the PS had four spills with a duration of 0.45 s (full time 1.8 s) at the best conditions. On the SPS the beam time during the same supercycle is 4.6*2 = 9.6 s. This gives a factor of 5 atom production per time unit at 450 GeV/c. With this additional increase the number of produced atoms at the same intensity of the secondary particles is more than an order of magnitude higher than at 24 GeV/c.

Note also that the soft proton background at 450 GeV/c is more than an order of magnitude lower than at 24 GeV/c [25, 27], thus decreasing by an order of magnitude the background of $p\pi^-$ pairs relative to the $K^+\pi^-$ pairs.

4.3. Calculations of the correlation function $R(\vec{p_1}, \vec{p_2}, s)$ at a proton momentum of 24 and 450 GeV/c for the π^+K^-, $K^+\pi^-$ and $\pi^+\pi^-$ pairs with a small relative momentum.

The differential inclusive yield of atom production in equation (4) is expressed in terms of the double differential yield of two constituent particles. We obtained this yield using

the FTF generator. We can also use the FTF to determine the correlation function from equation (5) which allows the uncertainty in the minimum value of W_A^N to be evaluated. This factor for the momentum interval of the DIRAC setup is presented in Fig.7. It shows that the factor R for $\pi^+\pi^-$ pairs at 24 GeV/c decreases from 1.25 (p_{pair} = 3 GeV/c) down to 0.5 ($p_{pair} = 9$ GeV/c). For $K\pi$ pairs R decreases from 1 (3 GeV/c) down to 0.5 (10 GeV/c). This decrease is partially due to conservation law constrains. The value of R at 450 GeV/c practically does not depend on the pair momentum and the polar angle.

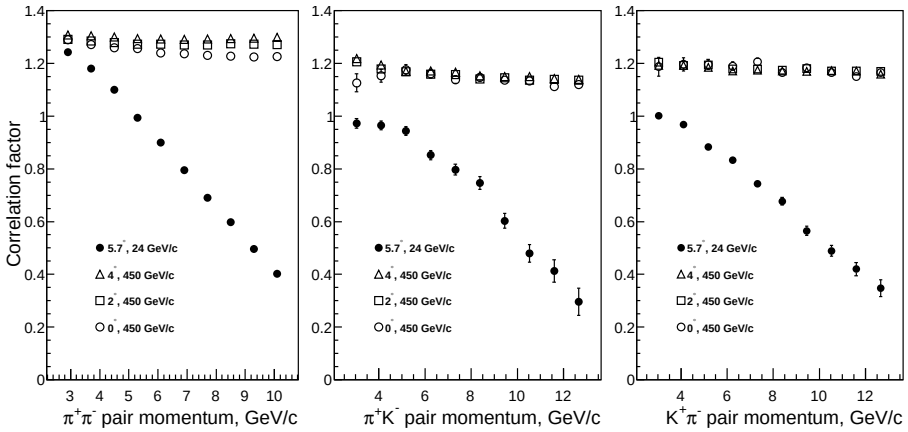

Figure 7. The dependence of correlation factor R for the $\pi^+\pi^-$, π^+K^- and $K^+\pi^-$ pairs in the DIRAC setup on their momentum in l.s. at 450 GeV/c and emission angles $\theta_{lab} = 0°$, 2°, 4° and at 24 GeV/c and the emission angle $\theta_{lab} = 5.7°$.

As we can see from Fig.7, the correlation function R for all kinds of pairs is smaller at 24 GeV/c than at 450 GeV/c for all pair momenta. The calculation of the relative atom yields W_A^N with $R = 1$ gives us the minimum value of W_A^N. In this case the error of W_A^N depends only on the uncertainties of the inclusive cross section description by the FTF. These uncertainties can be evaluated from the experimental data analysis.

4.4. The dependence of the atom and charged particle production on the target material.

There was studied the dependence of charged particle and atom yields on the target material. Three materials were used: Be, Ni and Pt. These yields for the case of charged particles are shown on Fig.8 as dependence on particle momentum at 450 GeV/c and $\theta_{lab} = 4°$. One can see that the yield of charged particles increases 1.8 times with growth of nucleus atomic number from Be to Pt.

The productions of atoms integrated over the setup momentum intervals at different target materials at 450 GeV/c and $\theta_{lab} = 4°$ are shown in Tab.3. One can see that the ratio of atom productions between Pt and Be is about 3 which is about the square of charged particle intensity ratio in accordance with the atom production equations (4) and (5).

Table 3. The yields $dN/dp[(GeV/c \times msr)^{-1}]$ of the $\pi^+\pi^-$, π^+K^- and $K^+\pi^-$ atoms at 450 GeV/c and an emission angle $\theta_{lab} = 4^\circ$ for the Be, Ni and Pt targets.

Atoms	Target		
	Be	Ni	Pt
$A_{2\pi}$	1.3×10^{-8}	1.9×10^{-8}	3.6×10^{-8}
$A_{K^-\pi^+}$	3.4×10^{-10}	8.8×10^{-10}	10.2×10^{-10}
$A_{K^+\pi^-}$	5.2×10^{-10}	9.7×10^{-10}	16.7×10^{-10}

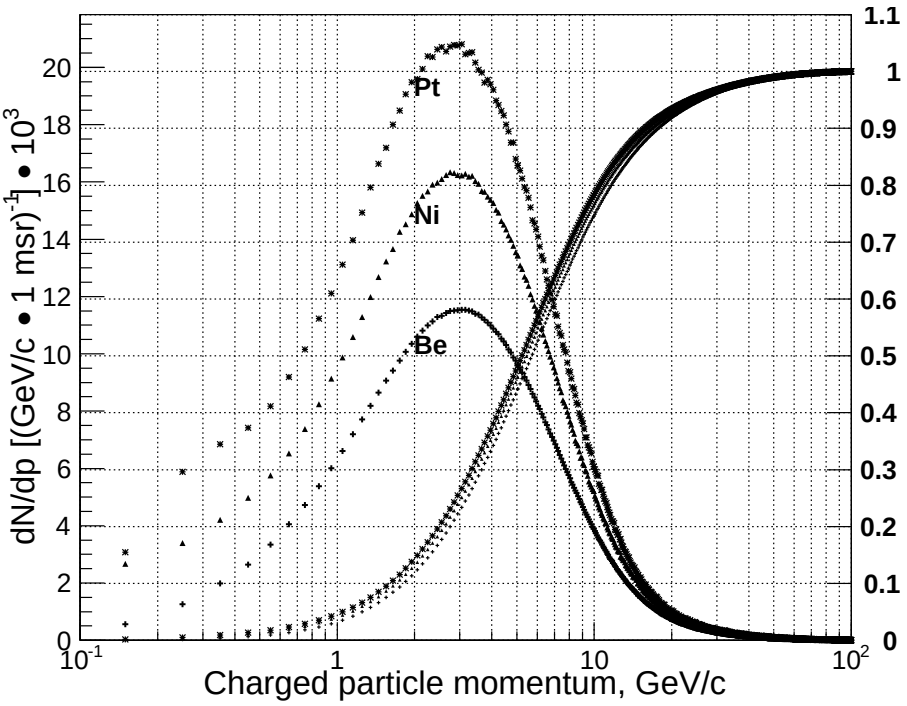

Figure 8. The total yield of the charged particles ($\pi^\pm$, $K^\pm$, p and $\bar{p}$) per p-nucleus (Be, Ni and Pt) interaction event at 450 GeV/c and an emission angles $\theta_{lab} = 4^\circ$ as a function of their momentum in l.s. for the solid angle of 10^{-3} sr. The integrated and normalized-to-unity distributions are also shown.

5. On the accuracy of the FTF simulation results.

In the equation (5) the double yield is presented via the product of two single particle yields and a correlation factor R. It was shown (chapter 4.3) that if $R = 1$ then the minimum relative yield value $W_A^N(R = 1)$ is reached. In this case the error in $W_A^N(R = 1)$ depends only on the uncertainty in the single particle yield description by FTF which we can obtain from experimental distributions (Fig.1-3).

The product of experimental π^+ and π^- distributions (Fig.1) in the corresponding intervals of momentum and polar angle were compared with MC distributions. The

dedicated correction factors and their errors were calculated [28]. These correction factors were used to estimate the minimal gain of atom production at 450 GeV/c relative to 24 GeV/c (Tab.4,5).

The $W_A(R=1)$ and $W_A^N(R=1)$ values are presented in Tab.4. At 450 GeV/c and $\theta_{lab} = 4^\circ$ the minimum ratios of $A_{2\pi}$, $A_{\pi^+K^-}$ and $A_{\pi^-K^+}$ equal to 9.7±1.5, 45±8 and 18.6±4.1 respectively confirming that even minimum yields of $A_{\pi^+K^-}$ and $A_{\pi^-K^+}$ at 450 GeV/c are more than by an order of magnitude larger that the yields at 24 GeV/c.

Table 4. The yield $W_A(R=1)$ of $\pi^+\pi^-$, π^+K^- and $K^+\pi^-$ atoms into the aperture of 10^{-3} *sr* with allowance for the setup acceptance and pion and kaon decays per pNi interaction event at 24 and 450 GeV/c versus the emission angle θ_{lab}. The ratio $W_A^N(R=1) = W_A(R=1,\ 450\ GeV/c)/W_A(R=1,\ 5.7^\circ, 24\ GeV/c)$ gives the minimum ratio of the atom yields at 450 GeV/c and 24 GeV/c.

θ_{lab}	5.7°	4°	2°	0°
E_p	24 GeV/c	450 GeV/c	450 GeV/c	450 GeV
Yield of $\pi^+\pi^-$ atoms				
$W_A(R=1)\times 10^9$	1.73±0.09	17±2	30±5	39±6
$W_A^N(R=1)$	1	9.7±1.5	17.5±2.8	22.7±3.6
Yield of π^+K^- atoms				
$W_A(R=1)\times 10^9$	0.015±0.001	0.66±0.11	1.31±0.21	1.52±0.24
$(W_A^N(R=1))$	1	45±8	87±15	104±18
Yield of $K^+\pi^-$ atoms				
$W_A(R=1)\times 10^9$	0.042±0.003	0.79±0.16	1.8±0.4	2.2±0.5
$W_A^N(R=1)$	1	18.6±4.1	41±9	52±11

6. The status of $\pi\pi$ and πK scattering length and prospect of their precision improvement.

In this chapter the best experimental data on $\pi\pi$ and πK scattering lengths, the most precise theoretical predictions of these parameters and prospect of the experimental data improvement at 450 GeV/c are presented.

6.1. The measurements and theoretical calculations of $\pi\pi$ scattering lengths.

The $\pi\pi$ s-wave scattering lengths a_0 and a_2 and their difference calculated with high precision [3], using Chiral Perturbation Theory (ChPT) [31, 32], are: $a_0 = 0.220 \pm 2.3\%, a_2 = -0.0444 \pm 2.3\%, |a_0 - a_2| = 0.265 \pm 1.5\%$. The large contribution to $\pi\pi$ scattering length errors give the constants l_3 and l_4. The constant l_3 was calculated [32] with a precision of about 100% and l_4 with a precision of about 25%. After 2006, these constants were obtained in many works using Lattice calculations. The best result has

Table 5. The relative yields $W_A(R=1)/W_{ch}$ of the $\pi^+\pi^-$, π^+K^-, and $K^+\pi^-$ atoms into the aperture of 10^{-3} sr with allowance for the setup acceptance and pion and kaon decays per pNi interaction event at 24 and 450 GeV/c versus the emission angle θ_{lab}. $(W_A(R=1)/W_{ch})^N$=$(W_A(R=1,450\ GeV/c)/W_{ch})/(W_A(R=1,5.7^\circ,24\ GeV/c)/W_{ch})$.

θ_{lab}	5.7°	4°	2°	0°
E_p	24 GeV/c	450 GeV/c	450 GeV/c	450 GeV
Yield of $\pi^+\pi^-$ atoms				
$W_A(R=1)/W_{ch}\times 10^9$	78±4	121±14	60±10	13.4±2.1
$(W_A(R=1)/W_{ch})^N$	1	1.55±0.20	0.77±0.13	0.17±0.03
Yield of π^+K^- atoms				
$W_A(R=1)/W_{ch}\times 10^9$	0.66±0.04	4.7±0.8	2.6±0.4	0.52±0.08
$(W_A(R=1)/W_{ch})^N$	1	7.±1.	3.9±0.7	0.79 ±0.13
Yield of $K^+\pi^-$ atoms				
$W_A(R=1)/W_{ch}\times 10^9$	1.91±0.14	5.6±1.1	3.6±0.8	0.76±0.17
$(W_A(R=1)/W_{ch})^N$	1	2.9±0.6	1.9±0.4	0.40±0.09

25% error in l_3 and 12% in l_4. Therefore the precision of ChPT predictions of $\pi\pi$ scattering lengths can be improved.

In some recent works [35–39] $\pi\pi$ scattering lengths were evaluated using Lattice calculations. In [35] $a_0 = 0.214 \pm 4\%$ and $a_2 = -0.04430 \pm 10\%$. The value and precision of a_2 in [36–38] is the same as in [35]. In [39] $a_0 = -0.04330 \pm 1\%$. Therefore the precise measurement of $\pi\pi$ scattering lengths will test also the QCD predictions.

At present time only $|a_0 - a_2|$ is measured [7,20] with a precision of about 4% which is worse than the theoretical accuracy 1.5%. Using proton beam of 450 GeV/c, the error in $|a_0 - a_2|$ without setup improvement will be at the level of 2.5%(1% - statistical and 2.3% - systematic and theoretical errors).

The high energy proton beam and the simple change of the experiment scheme [28] open a new possibility for the long-lived $\pi\pi$ atom investigation. It allows to measure the Lamb shift in this atom and to extract another combination of the $\pi\pi$ scattering length $2a_0 + a_2$. In the DIRAC experiment, $436 \pm 57stat \pm 23syst$ $\pi^+\pi^-$ atomic pairs from the breakup of long-lived atoms in the Pt foil were detected [9]. These atoms were created in Be target and spanned without decaying the distance of 96 mm between Be target and Pt foil. The main contribution to the statistical error comes from the background of $\pi^+\pi^-$ pairs generated in the Be target and their number is 40 times higher than the number of atomic pairs; the high background level has also a strong influence on the systematic error. In the new scheme [28] a collimator and magnet are installed after the target, deflecting charged particles generated in the target with the momentum less than 10 GeV/c. These particles will not be detected by the setup detectors behind the spectrometer magnet and the background will be decreased by two orders of magnitude

up to 10% of the number of atomic pairs . This background level was fixed in the work [33] which used the same scheme for the detection of $\pi\mu$ atomic pairs from $\pi\mu$ atom breaking in the thin foil. The magnet installation behind the Be target allows also to decrease the flux of secondary particles hitting forward detectors. Therefore the proton beam intensity can be increased by factor a 5(see Fig.8). In this scheme the number of produced $\pi^+\pi^-$, π^+K^- and $K^+\pi^-$ atoms per time unit increases by a factor of 60, 265 and 120 respectively. The number of $\pi^+\pi^-$ atomic pairs per time unit increases less than the number of atoms because the Pt foil must be installed after the magnet and part of the long-lived atoms will decay. Nevertheless, the statistics increasing and significant background suppression will allow to use the resonance method [16] for measurement of the one parameter, Lamb shift, and evaluate the combination of the $\pi\pi$ scattering lengths $2a_0 + a_2$.

In all other processes, where $\pi\pi$ scattering lengths are studied, the level of background is one order of magnitude larger than the effect and cannot be significantly suppressed due to physical reasons. The atomic pair number from short-lived $\pi\pi$ and πK atoms broken in the target is 15-20 times less than the background of free pairs, generated on the same target. This ratio cannot be decreased significantly because multiple scattering in the target and momentum resolution smear the atomic pairs distribution in the aria Q_t, Q_l where the number of free pairs is 15-20 times larger than the number of atomic pairs . For K decays the $\pi\pi$ interaction changes the experimental distributions calculated without taking into account a $\pi\pi$ interaction of about 10%. Therefore, the background is also one order of magnitude larger than the effects, in connection with $\pi\pi$ interaction.

The second property of the long-lived atoms is the absence of theoretical limitation of the results precision. For these atoms the energy splitting can be evaluated using only Lorenz transformation and quantum mechanics [28]. In this case the theoretical uncertainty of the strong part of energy splitting, in connection with $\pi\pi$ scattering lengths, will be of the level of 10^{-4} [34]. For all other processes analysis, we need theoretical relations with precision 10^{-2} in the best case. It gives the principal limit of this analysis accuracy.

It is important to stress that all experiments with dimesoatoms do not disturb the proton beam, because the nuclear efficiency of the targets is less than 10^{-3}.

6.2. The measurement and theoretical calculations of πK scattering lengths.

The measurements of s-wave $\pi\pi$ scattering lengths confirm our understanding of the chiral $SU(2)_L * SU(2)_R$ symmetry breaking of QCD with a precision of 4%. But these measurements, independently from their accuracy, cannot check our understanding of the chiral $SU(3)_L * SU(3)_R$ symmetry. This check can be done only by measuring of s-wave πK scattering lengths with s quark participating also. It is the principal difference between $\pi\pi$ and πK scattering lengths. The experimental value of πK scattering length combination evaluated from πK atom lifetime measurement [8] is $|a_{1/2} - a_{3/2}|$ =0.32

with an average precision of about 60%.

The ChPT in two-loop approximation [12] gives only $|a_{1/2} - a_{3/2}|$ =0.267 without a precision estimation. This value is 10% larger than the result obtained using one-loop approximation [11]. This difference can be used as the upper limit of the error of ChPT prediction in two-loop approximation for the $|a_{1/2} - a_{3/2}|$.

There is a good agreement between a Lattice calculation of πK scattering lengths [35, 36, 39]. In these works only $a_{1/2}$ and $a_{3/2}$ were calculated with statistical and systematic errors. The errors of $|a_{1/2} - a_{3/2}|$ presented in this paper are obtained as the square root of the sum of the squares of the scattering length errors. The relative difference between the values of $|a_{1/2} - a_{3/2}|$ =0.2331±2% [35] and =0.2432±2% [36] is about 4% in agreement with the errors presented. The accuracy of πK scattering lengths is significantly better than Lattice calculations of $\pi\pi$ scattering lengths. Therefore the πK scattering length measurement is the effective way to check the QCD precise predictions.

The experimental data on πK scattering at high energy were analyzed using Roy and Steiner type equations [10]. In this work the πK scattering lengths and and their difference: $|a_{1/2} - a_{3/2}| = 0.269 \pm 6\%$ were estimated with their uncertainties.

It is obvious that at the present time ChPT and Lattice calculation predictions were not checked by experimental measurements because the average error of $|a_{1/2} - a_{3/2}|$ in the DIRAC experiment is 60%. If the DIRAC setup would be installed on the proton beam of 450 GeV/c without any change then the statistics of πK atomic pairs would be increased about 36 times (see chapter 4.2) and $|a_{1/2} - a_{3/2}|$ would be measured with a precision of 9%, because there is a nonlinear dependence of $|a_{1/2} - a_{3/2}|$ error on the statistical error of atomic pair number. The setup upgrade and geometry modification will allow to improve this precision.

7. Conclusion

The performed analysis has shown that the dimesoatom production in the p-nucleus interaction can be increased by more than an order of magnitude if the incident proton momentum is changed from 24 GeV/c to 450 GeV/c. The yield of $A_{2\pi}$ ($A_{\pi^+K^-}$, $A_{\pi^-K^+}$) in the momentum interval of the DIRAC experiment p_A = 2.5-10.5 GeV/c (5-14 GeV/c) at 450 GeV/c and $\theta_{lab} = 4^\circ$ is 17 (38, 16) times higher than their production at 24 GeV/c and $\theta_{lab} = 5.7^\circ$ (Table 1). The yields are twice as high for $\theta_{lab} = 2^\circ$. All these values were calculated by integration of the dedicated atomic momentum spectrum in the intervals mentioned above. If one takes into account the DIRAC setup acceptance (Table 2), the relative yields of $A_{2\pi}$, $A_{\pi^+K^-}$ and $A_{\pi^-K^+}$ at $\theta_{lab} = 4^\circ$ (2°) at 450 GeV/c are 15(28), 67(131) and 31(68) times higher than at 24 GeV/c. The minimum values of these ratios were evaluated in the model-independent way and the following results (Table 4) were obtained at $\theta_{lab} = 4^\circ(2^\circ)$: 9.7±1.5 (17.5±2.8), 45±8 (87±15) and 18.6±4.1 (41±9). They confirm that even the minimum yields at 450 GeV/c are higher by more than an order of magnitude than at 24 GeV/c.

In the experiments on the lifetime measurement of short-lived $A_{2\pi}$, $A_{\pi^+K^-}$ and $A_{\pi^-K^+}$ the secondary particle flux intensity in the DIRAC experiment restricted the primary proton beam intensity and the number of detected atoms within a time unit. For the same total flux intensity of the charged particles as in the DIRAC experiment the yields of $A_{2\pi}$, $A_{\pi^+K^-}$ and $A_{\pi^-K^+}$ at 450 GeV/c and $\theta_{lab} = 4^\circ$ are 2.4, 10.6 and 4.9 times higher respectively. As mentioned in section 4.2, the beam time per supercycle on the SPS is 5 times higher than on the PS. Therefore the number of $A_{2\pi}$, $A_{\pi^+K^-}$, and $A_{\pi^-K^+}$ per time unit can be 12, 53 and 24 times higher respectively. The strong increasing of $A_{\pi^+K^-}$ and $A_{\pi^-K^+}$ statistics will allow to check for the first time our understanding of the chiral $SU(3)_L * SU(3)_R$ symmetry breaking of QCD.

In the DIRAC experiment, 436±57stat±23syst $\pi^+\pi^-$ atomic pairs from the breakup of long-lived atoms in the Pt foil were detected [9]; these atoms were created in the Be target. The main contribution to the statistical error comes from the background of $\pi^+\pi^-$ pairs generated in the Be target which is 40 times higher than the number of atomic pairs. It was discussed [28] that the magnet installation behind the Be target allows the proton beam intensity to be increased by factor 5(see Fig.8) and the background to be decreased by about two orders of magnitude. In this scheme the number of produced $\pi^+\pi^-$, π^+K^-, and $K^+\pi^-$ atoms per time unit increases by a factor of 180, 800 and 370 respectively. The large statistics and significant background suppression will allow to use the resonance method [16] for measurements of the Lamb shift and combination of $\pi\pi$ scattering lengths $2a_0 + a_2$. This analysis involves only the Lorentz transformation and quantum mechanics.

The all experiments with dimesoatoms do not disturb the proton beam because the nuclear efficiency of the targets is less than 10^{-3}.

8. Acknowledgments

We are grateful to M.Gadzitski and A.Korzenev for providing us with the unpublished data on inclusive cross sections for pC interactions at 31 GeV/c. We are also grateful to V.Uzhinsky for the discussion on the FTF generator and to D.Drijard, P.Shcliapnikov and V.Yazkov for helpful comments.

[1] J.Uretsky and J.Palfrey, Phys. Rev. **121** (1961) 1798.
[2] S.M.Bilenky et al., Yad. Phys. **10** (1969) 812; (Sov. J. Nucl. Phys. **10** (1969) 469).
[3] J. Gasser et al., Phys. Rev. **D64** (2001) 016008; he*p*-ph/0103157.
[4] J.Schweizer, Phys. Lett. **B587** (2004) 33. J. Schweizer, Eur.Phys.J. C 36 (2004) 483, arXiv:hep-ph/0405034.
[5] A.Adeva et al., J. Phys. G: Nucl. Part. Phys. **30** (2004) 1929.
[6] B.Adeva at al., Phys. Lett. **B619** (2005) 50.
[7] A.Adeva et al., Phys. Lett. **B704** (2011) 24.
[8] A.Adeva et al., Phys. Lett. **B735** (2014) 288.
[9] A.Adeva et al., Phys. Lett., **B751** (2015) 12., arXiv:1508.04712.
[10] P.Buttker, S.Descotes-Genon, B.Moussallam, Eur. Phys. J. **c33** (2004) 409. J. High Energy Phys. **O405**(2004) 036 he*p*-ph/0404150.
[11] V.Bernard et al., Nucl. Phys. **B357** (1991) 129., Phys. Rev. **D43** (1991) 3557.
[12] J.Bijnens et al., J. High Energy Phys. **O405**(2004) 036 hep-ph/0404150.

[13] C.B.Lang, et al., Phys. Rev. **D86** (2012) 054508.
[14] L.Nemenov, Yad. Fiz. **41** (1985) 980.
[15] L.L.Nemenov and V.D.Ovsiannikov, Phys. Lett. **B514** (2001) 247.
[16] L.L.Nemenov, V.D.Ovsyannikov, E.V.Chaplygin, Nucl. Phys. **A710** (2002) 303.
[17] G.V.Efimov at al.,Yad.Fiz.44(1986),460;(Sov.J.Nucl.Phys. 44 (1986) 296.
[18] A.Karimhodjaev and R.N.Faustov,Yad.Fiz.29 (1979) 463;Sov.J.NuclPhys. 29 (1979) 232.
[19] J.R.Bateley at al., Eur. Phys. J. **C64** (2009) 589.
[20] J.R.Bateley at al., Eur. Phys. J. **C70** (2010) 635.
[21] V.Uzhinsky, arXiv:1109.6768[hep-ph], 2011.
[22] S. Agostinelli et al., NIMPA **506** (2003) 250.
[23] N.Abgrall at al , Phys.Rev C84 034604(2011), Phys.Rev. **C85** 035210(2012), Private communication.
[24] D.S.Barton at al.,Phys. Rev. **D27** (1983) 2580.
[25] G.Ambrosini at al.,Eur.Phys.J. **C10** (1999) 605.
[26] Grishin V.G., Inclusive processes in hadron interactions at high energy. Energoizdat, Moscow 1982, p. 131 (in Russian).
[27] Eichten T. et al., Nucl. Phys. **B44** (1972) 333.
[28] O.Gorchakov and L.Nemenov[JINR], DIRAC Note **2015-5**.
[29] O.Gorchakov and L.Nemenov[JINR], DIRAC Note **2015-3**.
[30] O.Gorchakov and L.Nemenov[JINR], DIRAC Note **2012-6**.
[31] S.Weinberg, Physica **A96** (1979) 327.
[32] J.Gasser and H.Leutwyiler, Nucl. Phys. **B250** (1985) 465.
[33] S.H.Aronson et al.,Phys. Rev. Lett. **48** (1982) 1078-1081.
[34] S.Karshenboim, privet communication.
[35] Z.Fu, Phys.Rev. **D87**, 084501 (2013).
[36] K.Sasaki et al.,Phys.Rev. **D89**, 054502(2014).
[37] X.Feng, K.Jansen, and D.Renner, Phys. Lett. **B684**, 268 (2010).
[38] T.Yagi at al., arXiv: 1108.2.
[39] S.R.Beane et al., Phys.Rev. **D77**, 014505(2008).